

Local Voting: A New Distributed Bandwidth Reservation Algorithm for 6TiSCH Networks

Dimitrios J. Vergados^{a,*}, Katina Kralevska^b, Yuming Jiang^b,
Angelos Michalas^a

^a*Dep. of Informatics, University of Western Macedonia, Kastoria, Greece*

^b*Dep. of Information Security and Communication Technology, NTNU,
Norwegian University of Science and Technology*

Abstract

The IETF 6TiSCH working group fosters the adaptation of IPv6-based protocols into Internet of Things by introducing the 6TiSCH Operation Sublayer (6top). The 6TiSCH architecture integrates the high reliability and low-energy consumption of IEEE 802.15.4e Time Slotted Channel Hopping (TSCH) with IPv6. IEEE 802.15.4e TSCH defines only the communication between nodes through a schedule but it does not specify how the resources are allocated for communication between the nodes in 6TiSCH networks. We propose a distributed algorithm for bandwidth allocation, called Local Voting, that adapts the schedule to the network conditions. The algorithm tries to equalize the link load (defined as the ratio of the queue length plus the new packet arrivals, over the number of allocated cells) through cell reallocation by calculating the number of cells to be added or released by 6top. Simulation results show that equalizing the load throughout 6TiSCH network provides better fairness in terms of load, reduces the queue sizes and packets reach the root faster compared to representative algorithms from the literature. Local Voting combines good delay performance and energy efficiency that are crucial features for Industrial Internet-of-Things applications.

Keywords: IoT, IEEE 802.15.4e, 6TiSCH, networks, TSCH, 6top,

*Corresponding author

Email addresses: dvergados@uowm.gr (Dimitrios J. Vergados), katinak@ntnu.no (Katina Kralevska), jiang@ntnu.no (Yuming Jiang), amichalas@uowm.gr (Angelos Michalas)

1. Introduction

Wireless Sensor Networks (WSNs) have advanced significantly in the past decades. The recent increase of connected devices has triggered countless Internet-of-Things (IoT) applications to emerge [1]. It is expected that 50 billion devices will be connected to the Internet by 2020 [2]. The so-called Industrial Internet-of-Things (IIoT) is modernizing various domains such as home automation, transportation, manufacturing, agriculture, and other industrial sectors.

Often IoT is realized through Low-power and Lossy Networks (LLNs), which consist of low complexity resource constrained embedded devices, that are interconnected using different wireless technologies. The IEEE 802.15.4e standard defines the physical and the medium access control (MAC) layers for ultra-low power and reliable networking solutions for LLNs [3]. There are five MAC modes: Time Slotted Channel Hopping (TSCH), Deterministic and Synchronous Multi-channel Extension (DSME), Low Latency Deterministic Network (LLDN), Asynchronous Multi-Channel Adaptation (AMCA), and Radio Frequency Identification Blink (BLINK) [4]. In this work, we study TSCH which is designed to allow IEEE 802.15.4 devices to support a wide range of applications, including industrial ones. In industrial environments, the large metallic equipment causes multi-path fading and interference [5], and TSCH combats against them by combining channel hopping and time synchronization. The channel hopping allows transmissions between nodes to use different channels, while the slotted access enhances the reliability by synchronizing the nodes with a schedule and, thus, avoiding collisions.

The IETF 6TiSCH working group standardizes the protocol stack for IIoT [6]. It combines the high reliability and the low-energy consumption of IEEE 802.15.4e TSCH with the addressability and Internet integration capabilities of Internet Protocol version 6 (IPv6). The communication in a 6TiSCH network is orchestrated by a schedule composed of cells, where each cell is identified by [slotOffset,

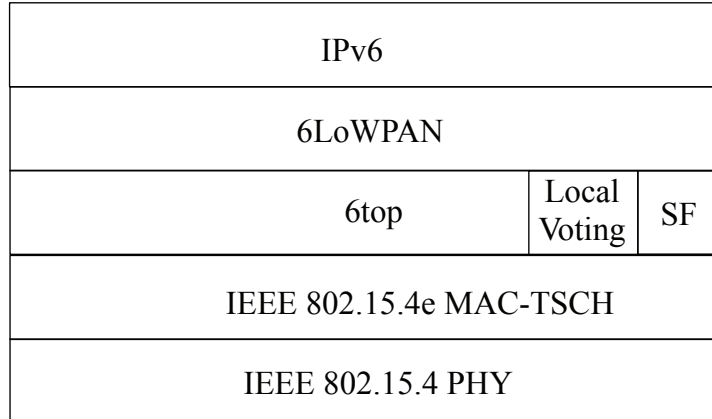


Figure 1: The 6TiSCH protocol stack. We propose an algorithm for bandwidth reservation, called Local Voting, that is located in the 6top sublayer.

channelOffset] [7]. The schedule specifies the channel (based on the channelOffset) and the time slot (based on the slotOffset) for communication of a node with each of its neighbors. The IEEE 802.15.4e standard defines how the schedule is executed but it does not define how the schedule is built and updated. Fig. 1 shows the 6TiSCH protocol stack where the 6TiSCH Operation Sublayer (6top) integrates the IEEE 802.15.4e MAC-TSCH layer with the IPv6-enabled upper stack [7]. The roles of the 6top sublayer are:

- to terminate the 6top Protocol (6P), which allows a node to communicate with a neighboring node to add/delete cells;
- to run one or multiple 6top scheduling functions (SF), which define the rules when to add/delete cells between neighboring nodes while monitoring performance and collecting statistics.

The biggest challenges for enabling the pervasive deployment of IoT devices are the demand for high reliability and the limited energy supply for the nodes. These challenges are magnified with the increase of the number of network devices and the emergence of new applications with diverse requirements. As the deployment cases become more dense, and new applications and devices

are added, the traffic patterns become more congested. In these conditions, we have found that the network performance is determined by the ability of the network to distribute the resources (cells) among the competing links, in a way that maximizes efficiency [8, 9].

In this paper, we propose a distributed bandwidth reservation algorithm called *Local Voting* (LV). It balances the load between the links in the network, where the load is defined as the ratio of the queue length plus new packet arrivals, over the number of allocated cells. LV was originally proposed in [8] in the context of wireless mesh networks. Here we adapt the above algorithm for the link-based multi-channel environment of 6TiSCH networks. Through analysis and extensive performance evaluation we show here that by redistributing cells among the links, we can limit the maximum delay in the network, and at the same time enhance reliability and fairness at a lower energy cost compared to scenarios where no load balancing takes place.

Most of the related works focus on ways to construct an optimal schedule between the links, without taking into consideration the optimal number of cells that should be allocated to each link. These works usually consider the On-The-Fly (OTF) bandwidth reservation algorithm [10]. Using the OTF algorithm, each node in the network estimates the number of cells that it requires for fulfilling its communication requirements by estimating the amount of new and forwarded traffic that it needs to transmit to its parent nodes. Then, the OTF module asks the 6top sublayer to add or remove cells, in order for the allocation to match this number if possible. However, the OTF algorithm does not consider the case where the requested number of cells exceeds the number of available cells, due to congestion. The nodes under OTF also do not consider the traffic requirements of the neighboring nodes, so there is no provision for cell redistribution to neighbors with higher bandwidth demands. Finally, the OTF algorithm tries to maintain a stable schedule by using a long-term average of the estimated throughput, which leads to inefficient allocation when the traffic patterns fluctuate. For these reasons we introduce LV algorithm that addresses the above limitations of OTF. We compare a thorough performance comparison

between two versions of LV and OTF and Enhanced-OTF (E-OTF) [11]. Under LV, information about the queue lengths and the cell allocations are periodically diffused among neighboring nodes, which use this information to calculate the number of cells that should be allocated to each link based on the load of each interfering link. Equalizing the load throughout the congested areas in the network leads to better fairness in terms of load for LV compared to OTF and E-OTF. The performance evaluation also shows that LV provides similar performance in terms of delay to E-OTF with an energy consumption similar to OTF, making LV a promising distributed bandwidth reservation algorithm for 6TiSCH networks.

The rest of the paper is organized as follows. Section 2 summarizes the related works. In Section 3, the network model is formulated. Section 4 presents Local Voting algorithm. Extensive performance evaluation results are presented in Section 5, and Section 6 concludes the paper.

2. Related Works

2.1. 6TiSCH scheduling protocols

Recently there have been many proposals for centralized and distributed solutions for TSCH scheduling in the literature. Centralized algorithms designate a specific scheduling entity that collects information about the network and adjusts the TSCH schedule to it. The first proposed centralized algorithm is Traffic Aware Scheduling Algorithm (TASA) [12], which builds a time/frequency collision-free schedule in a centralized manner. A master node collects information about the entire network topology and the load of each node. Then, it computes the schedule by exploiting matching and coloring procedures. The main disadvantages of centralized scheduling techniques is the signaling overhead since each node in the network has to communicate with the scheduler, there is a single point of failure, and there is a limit on the size of the topology since the scheduler becomes a bottleneck of the scheduling function.

As a counterpart, distributed approaches have been proposed where nodes agree on the schedule by applying distributed scheduling protocols and neighbor-to-neighbor negotiation, without having a central entity. The first distributed scheduling algorithm was proposed in [13], and it has been followed later by numerous algorithms. Decentralized traffic aware scheduling (DeTAS) [14] uses a hierarchical approach where all nodes follow a macro schedule that is a combination of micro-schedules for each routing graph. Orchestra [15] is the first algorithm towards autonomous scheduled TSCH where nodes compute their own schedule locally and autonomously based on the routing layer information.

At the MAC layer, decentralized scheduling results in cell overlapping and thus in many collisions. A collision occurs when the same cell is allocated to different pairs in the same interference range. In order to avoid cell overlapping and reduce internal interference, Decentralized Broadcast-based Scheduling algorithm (DeBraS) [16] allows nodes to share scheduling information. The collision reduction and throughput improvement by DeBraS for dense networks come at the cost of higher energy consumption.

The algorithm proposed in [17] allows every sensor node to compute its time-slot schedule in a distributed manner. A scheme called Reliable, Efficient, Fair and Interference-Aware Congestion Control (REFIACC) [18], takes into account the heterogeneity in link interference and capacity when constructing the scheduling send policy in order to reach the maximum fair throughput in wireless sensor networks. The authors in [19] proposed a "housekeeping" mechanism which detects scheduled collisions and reallocates each colliding cell to a different position in the schedule. A distributed cell-selection algorithm for reducing scheduling errors and collisions is proposed in [20]. It considers a fixed queue length, thus, the algorithm cannot adapt to the network conditions.

Wave [21] builds the schedule by constructing a series of waves in order to minimize the delay in convergecast applications. All successive waves are copies of the first wave, where slots without scheduled transmissions are removed. An extension of Wave, where subsequent waves overlap, has been presented in [22].

Recently, Decentralized Adaptive Multi-hop scheduling for 6TiSCH Net-

works (DeAMON) [23] and Recurrent Low-Latency Scheduling Function (ReSF) [24] have been proposed. ReSF minimizes the latency by reserving minimal-latency paths from the source to the sink, and it only activates these paths when recurrent traffic is expected. This results into a latency improvement of up to 80% compared to state-of-the-art low-latency scheduling functions. This improvement comes on the cost of an increased power consumption.

2.2. 6TiSCH bandwidth reservation algorithms

On-the-fly (OTF) [10] is a distributed algorithm that dynamically adapts the bandwidth allocation by calculating the number of cells to be added or removed according to a neighbor-specific threshold. OTF is prone to schedule collisions since nodes might not be aware of which cells are allocated to other pairs of nodes.

The authors in [11] assess the performance of OTF in terms of reliability and latency. In their assessment they focus on the impact of the network dynamics on the OTF performance, namely the routing protocol and the 6top negotiations. Based on their analysis, they propose Enhanced-OTF (E-OTF) which improves the OTF performance by modifying the allocation algorithm in OTF. First, E-OTF considers the channel quality in the computation of resources by introducing a measure for the average number of required retransmissions for a successful packet transmission. Second, it includes a mechanism to recover from congestion by taking into consideration the amount of queued data. However, E-OTF does not consider the energy consumption, that is one of the main requirements for efficient resource allocation algorithms for IoT devices.

Scheduling Function Zero (SF0) [25] adapts dynamically the number of reserved cells between neighboring nodes based on the application's bandwidth requirements and the network conditions. SF0 uses Packet Delivery Rate (PDR) statistics to reallocate cells when the PDR of one or more cells is much lower than the average PDR. Cost-aware cell relocation (CCR) [26] complements SF0 by detecting scheduling collisions and relocating the involved cell. To detect collisions, CCR compares the PDR of all cells to a particular neighbor. If one

cell has a PDR significantly lower than the PDR of other cells, then there is a schedule collision and that cell is relocated to a different slot/channel in the TSCH schedule.

References [27, 28, 29] provide an extended literature overview of scheduling algorithms in IEEE 802.15.4e.

In contrast to the related works, this paper introduces congestion control to the scheduling algorithm, in a way that leads to optimal performance in terms of delay. Specifically, the local voting mechanism is used for determining how many cells should be allocated to each link, not only based on its own traffic requirements, as other schemes already do, but also considering the traffic requirements and allocations of the neighboring (conflicting) links. This algorithm allocates the cells in a way that minimizes the maximum value of the ratio of queue length over number of cells (the load). Since the delay per link is given by this ratio, the allocation ensures the minimum delay per link under congestion.

3. Network Model and Problem Formulation

Our model considers a 6TiSCH network which has built a tree routing topology with one or multiple parents per node, using the Routing Protocol for Low-Power and Lossy Networks (RPL) [30]. For reader's convenience, Table 1 summarizes the notation used throughout this paper.

The communication in the network can be modeled by a graph $\mathcal{G} = (V, E)$, where $V = \{n_i : 0 \leq i < N\}$ is the set of all nodes and E is the set of edges that represent the communication symmetric links between the nodes. Data is gathered over a tree structure $\mathcal{G}_T = (V_T, E_T)$ rooted at the sink node n_0 where $n_0 \in V_T, V_T \subseteq V$, and $E_T \subseteq E$. We consider both of the cases where each node has only one parent (tree) and where there are multiple parents per node. Without loss of generality, we consider a single-sink model. We assume that all nodes are synchronized, and each node has a single half-duplex radio transceiver. Since the communication is half-duplex, each node cannot transmit and receive

Table 1: List of notations

$\mathcal{G} = (V, E)$	Network topology graph where V is the set of all nodes and E is the set of edges between the nodes
N	Total number of nodes in the network
$\mathcal{G}_T = (V_T, E_T)$	Tree topology graph where $V_T \subseteq V$ and $E_T \subseteq E$
n_0	Sink node, $n_0 \in V_T$
n_i	i -th node in the network, $n_i \in V, 1 \leq i < N$
f	Slot frame
S	Total number of time slots in a slot frame
t	Time slot where $0 \leq t < S$
M	Total number of channel offsets
$chOf$	Channel offset where $0 \leq chOf < M$
$c_{(i,j)}^{(t, chOf)}$	Cell with coordinates $(t, chOf)$ assigned to link (i, j)
$N_i^{(1)}$	Set of one-hop neighbors of node n_i
$N_{i,j}$	Set of all links that could interfere with link (i, j)
$q_{(i,j)}^f$	Number of packets that n_i sends to n_j at frame f
$p_{(i,j)}^f$	Number of allocated cells to link (i, j) at frame f
$z_{(i,j)}^f$	Number of new packets received by n_i with destination n_j at frame f
$u_{(i,j)}^f$	Number of cells added/deleted to link (i, j) at frame f due to Local Voting
$r_{(i,j)}^f$	Number of cells released from link (i, j) at frame f
$x_{(i,j)}^f$	Load of link (i, j) at frame f
$\tilde{N}_{(l,k)} \subset N_i^{(1)}$	Set of neighboring links of link (l, k) , that can give at least one cell to link (l, k)

simultaneously on the same channel. We propose a *link scheduling* algorithm where a link (i, j) is a pairwise assignment of a directed communication between a pair of nodes (n_i, n_j) , where $i \neq j$, in a specific time slot within a given frame and a channel.

Time in TSCH is slotted, and assumed to be (almost) perfectly synchronized in the whole system. The basic time interval is referred to as a time slot t . A time slot t is long enough for one packet to be sent from node n_i to node n_j and optionally node n_j to reply. This is represented in Fig. 2 for the node pair (n_3, n_1) . Each frame f consists of equal number of S time slots with the same duration $f = \{0, \dots, S - 1\}$. The resource allocation in a 6TiSCH network is controlled by a TSCH schedule that allocates cells for node communication. A cell represents a unit of bandwidth that is allocated based on a decision by a centralized or a distributed scheduling algorithm. As explained previously, a cell is defined by a pair of time slot and channel offset [31]. The slot offset is equal to time slot t while the channel offset $chOf$ is translated into a frequency with the following equation:

$$channel = F((chOf + ASN) \bmod M), \quad (1)$$

where $chOf$ denotes the channel offset, ASN counts the number of time slots since the network started, M is the number of physical channels (by default 16 in TSCH), and \bmod is the modulo operator. $F(\cdot)$ is a bijective function mapping an integer comprised between 0 and 15 into a physical channel. The number of channel offsets is equal to the number of available frequencies $0 \leq chOf < M$. The schedule can be represented by a matrix with dimensions: the total number of channel offsets M and total number of time slots in a slot frame S . One example of a schedule with 4 time slots and 3 channels is given in Fig. 2. Note that some cells can be shared between different links (e.g. $n_8 \rightarrow n_5$ and $n_6 \rightarrow n_4$), as long as there is no mutual interference. A TSCH schedule instructs node n_i what to do in a specific time slot and frequency: transmit, receive, or sleep. The cell assigned to link (i, j) at slot offset t and channel offset $chOf$ is

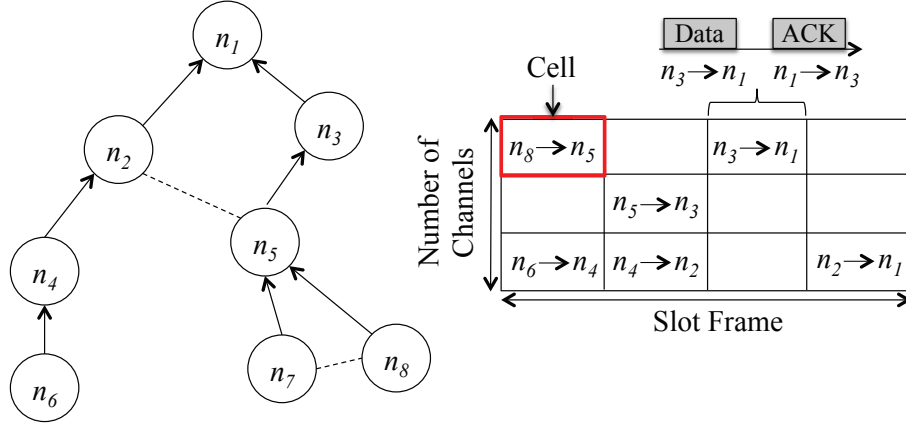


Figure 2: TSCH schedule for the presented topology where solid lines represent connection between nodes based on RPL and dashed lines represent possible communication between nodes.

denoted by $c_{(i,j)}^{(t, chOf)}$ where

$$c_{(i,j)}^{(t, chOf)} = \begin{cases} 1, & n_i \text{ transmits and } n_j \text{ receives at } t \text{ and } chOf; \\ 0, & \text{otherwise;} \end{cases} \quad (2)$$

for $n_i \in V, 0 \leq t \leq S - 1$, and $0 \leq chOf \leq M - 1$.

There exists a scheduled cell for node n_j from the pair (n_i, n_j) such that n_j receives the transmission from n_i at the same t and $chOf$ that are scheduled for transmission of node n_i . Each scheduled cell is an opportunity for node n_i to communicate with its one-hop neighbor n_j where $n_j \in N_i^{(1)}$ and $N_i^{(1)}$ denotes the one-hop neighborhood of node n_i . We consider an interference model where two nodes are one-hop neighbors as long as their Packet Delivery Rate (PDR) is larger than 0. In real scenarios, nodes that are at more than two hops distance can also interfere but with lower probability [32], thus, we only consider the one-hop neighborhood.

The 6top sublayer qualifies each cell as either a hard or a soft cell. A soft cell can be read, added, removed, or updated by the 6top sublayer, while a hard cell is read-only for the 6top sublayer. In the context of the proposed algorithm, all reallocated cells are soft cells.

The role of the bandwidth reservation algorithm is to ensure that there are enough resources to meet the application requirements such as traffic load, end-to-end delay, and reliability. The proposed scheduling algorithm must satisfy the following communication conditions:

1. Multi-point to point communication where data is generated only by source nodes n_i , where $n_i \in V_T$, and it is gathered at the sink node n_0 .
2. The communication is half-duplex, thus, each node cannot transmit and receive simultaneously on the same channel.
3. Nodes n_i and n_j from the pair (n_i, n_j) transmit and receive in the same cell, i.e., $(t, chOf)$, respectively.
4. *Collision-free* communication: A cell with coordinates $(t, chOf)$ is allocated to link (i, j) such that exactly one of the neighbors, i.e., node n_i , of the receiving node n_j should transmit at slot offset t and channel offset $chOf$, and the other neighbors n_l of the receiving node n_j , where $n_l \in N_j^{(1)}$ and $n_l \neq n_i$, might receive at slot offset t and channel offset $chOf$.

In general, to prevent collisions between pairs of links (i, j) and (l, k) , the following *collision-free* constraints are defined.

Primary conflict constraint: A node cannot transmit and/or receive two packets at the same time slot t , even not on different channels $chOf1$ and $chOf2$, i.e.,

$$c_{(i,j)}^{(t, chOf1)} c_{(l,k)}^{(t, chOf2)} = 0, \text{ for all: } \{i, j\} \cap \{k, l\} \neq \emptyset, \quad (3)$$

$$n_k \in N_i^{(1)}, n_l \in N_j^{(1)}.$$

Eq. (3) indicates that the communication is half-duplex.

Secondary conflict constraint: A receiver cannot decode an incoming packet in a channel $chOf$, if another node in its neighborhood is also transmitting at the same channel $chOf$ at the same time slot t . Hence, a node is not allowed to receive more than one transmission simultaneously, i.e.,

$$c_{(i,j)}^{(t, chOf)} c_{(l,k)}^{(t, chOf)} = 0, \text{ for all: } n_k \in N_i^{(1)}, n_l \in N_j^{(1)}. \quad (4)$$

Eq. (4) indicates the interference constraint.

4. Local Voting Bandwidth Reservation Algorithm

Each source node n_i , where $n_i \in V_T$ and $n_i \neq n_0$, has a queue with packets to be transmitted to the root through a parent node, which is a one-hop neighbor of the node n_i . The internal scheduling on the queue is first-come-first-serve. A cell is allocated to link (i, j) so that node n_i transmits a packet to n_j as it is given in Eq. (2).

The state of link (i, j) , where $n_j \in N_i^{(1)}$, at the beginning of frame $f + 1$ is described by three characteristics:

- $q_{(i,j)}^{f+1}$ is the number of packets (queue length) that node n_i has to transmit to node n_j at slot frame $f + 1$;
- $p_{(i,j)}^f$ is the number of cells allocated to link (i, j) at the previous slot frame f , i.e., $p_{(i,j)}^f = \sum_{t=0}^{S-1} c_{(i,j)}^{(t, chOf)}$.

There is no sum over the channels in the equation for calculating $p_{(i,j)}^f$ due to the fact that each node has a single transceiver, so each link can be allocated only one channel at each time slot.

The dynamics of each link (i, j) are calculated as:

$$\begin{aligned} q_{(i,j)}^{f+1} &= \max\{0, q_{(i,j)}^f - p_{(i,j)}^{f+1}\} + z_{(i,j)}^f, \\ p_{(i,j)}^{f+1} &= p_{(i,j)}^f + u_{(i,j)}^{f+1}, \end{aligned} \tag{5}$$

where

- $z_{(i,j)}^f$ is the number of new packets received from upper layers or from neighboring nodes of node n_i with a next-hop destination equal to node n_j at frame f ;
- $u_{(i,j)}^{f+1}$ is the number of cells that are added or released to link (i, j) at frame $f + 1$ due to LV.

The objective of the proposed LV algorithm is to schedule link transmissions in such a way that the minimum maximal (min-max) link delay is achieved. The algorithm stems from the finding that the shortest delivery time is obtained when the load is equalized throughout the network. The finding has been proved in [33] for the case of load balancing in cluster computing, while [8] presents a similar result for the case of wireless mesh networks with a single channel and a node scheduling MAC layer. In this paper we extend the result for link scheduling where the MAC layer follows TSCH mode.

The load of link (i, j) at frame f is defined as the ratio of the queue length $q_{(i,j)}^f$ over the number of allocated cells $p_{(i,j)}^f$ as follows:

$$x_{(i,j)}^f = \begin{cases} \left\lceil \frac{q_{(i,j)}^f}{p_{(i,j)}^f} + 0.5 \right\rceil, & \text{if } q_{(i,j)}^f > 0, \\ 0, & \text{if } q_{(i,j)}^f = 0, \end{cases} \quad (6)$$

where $\lceil \cdot \rceil$ is the round function (rounds a real number to the nearest integer). Note that by construction of the above definition, the delay at each link (i, j) (in time slots) can be computed as $x_{(i,j)} \cdot |S|$, where S is the number of slots in a slot frame.

In order to semi-equalize or balance the load in the network, neighboring links can exchange cells as long as Eq. (3) and Eq. (4) are satisfied. The set $N_{i,j}$ contains all links that could potentially interfere with link (i, j) . This means that

$$(l, k) \in N_{i,j} \text{ iff } n_k \in N_i^{(1)} \vee n_l \in N_j^{(1)}.$$

Definition 1. *A conflict-free schedule is link-wise optimal or just optimal, if the maximum delay per link in the network is smaller or equal than the maximum delay per link for every other schedule (min-max).*

Lemma 1. *(Optimal schedules are maximal) An optimal schedule is a (or has an equivalent) maximal schedule in the sense that¹ $\nexists(i, j) \in E$ such that $p_{(i,j)}$ can be increased without reducing $p_{(l,k)}$ for at least one other link where $(l, k) \in E$.*

¹Symbol \nexists denotes the negation of existence \exists

Proof: Consider a schedule that is not maximal. That means there exists $(i, j) \in E$ such that $p_{(i,j)}$ can be increased by one. Cells are not reallocated to other links, therefore, for the new schedule, the delay for all the other links is unchanged. For link (i, j) , the new delay is $x'_{(i,j)} \cdot |S| = \left[\frac{q_{(i,j)}}{p_{(i,j)}+1} + 0.5 \right] \cdot |S| \leq x_{(i,j)} \cdot |S|$. It follows that, for every non-maximal schedule, there exists a maximal schedule that has smaller or equal maximum delay. ■

Lemma 2. (*Optimal schedules are balanced*) Assume that link (l, k) is the most loaded link in the network, i.e., $(l, k) = \operatorname{argmax}(x_{(i,j)}), (i, j) \in E$. For all optimal schedules, it holds that $x_{(l,k)} \leq x_{(i,j)} / (1 - 1/p_{(i,j)})$ for the load of the most loaded link (l, k) and the load of every other link (i, j) , where $(i, j) \in \tilde{N}_{(l,k)}$, and $\tilde{N}_{(l,k)}$ is the set of neighboring links of link (l, k) that can give at least one cell to link (l, k) , without violating the constraints from Eq. (3) and Eq. (4).

Proof: Assume that an optimal schedule exists where for the most loaded link (l, k) , $x_{(l,k)} > x_{(i,j)} / (1 - 1/p_{(i,j)})$ where $(i, j) \in \tilde{N}_{(l,k)}$. Since (l, k) is the most loaded link, the maximal delay for such a schedule is $x_{(l,k)} \cdot |S|$. Since link $(i, j) \in \tilde{N}_{(l,k)}$, it follows that a cell of link (i, j) can be reassigned to link (l, k) . After reassigning, the new load for link (l, k) is $x'_{(l,k)} = [q_{(l,k)} / (p_{(l,k)} + 1) + 0.5]$, and the corresponding delay for link (l, k) is $[q_{(l,k)} / (p_{(l,k)} + 1) + 0.5] \cdot |S| < x_{(l,k)} \cdot |S|$. In addition, link (i, j) loses a cell so the new delay for link (i, j) is $[q_{(i,j)} / (p_{(i,j)} - 1) + 0.5] \cdot |S| = [(q_{(i,j)} / p_{(i,j)}) / (1 - 1/p_{(i,j)}) + 0.5] \cdot |S| = [(q_{(i,j)} / p_{(i,j)}) + 0.5] / (1 - 1/p_{(i,j)}) \cdot |S| = x_{(i,j)} / (1 - 1/p_{(i,j)}) \cdot |S| < x_{(i,j)} \cdot |S|$. Thus, the new allocation has a maximal delay that is smaller than or equal to the maximal delay of the other allocation, so the allocation is not optimal. ■

Based on the above reasoning, we design a load balancing strategy with two goals:

1. the produced schedule should be maximal; and
2. the load in the schedule should be balanced.

It should be noted that, in general, a schedule could be both maximal and balanced, but still not optimal. This is because there could exist a realloca-

tion of the slots in the network that would produce a larger spectral efficiency. Optimizing the schedule in this sense would require finding a solution for the *NP*-complete link scheduling problem. This is not easy, so for the purposes of this paper, we do not examine ways of escaping local optima and finding the global optimum. However, the simulation results show that the performance of LV is still better than the performance of the algorithms that we compare with, and that optimizing the maximal nodal delay also has a positive impact on the end-to-end delay.

In the following part we explain LV and the way how $u_{(i,j)}^{f+1}$ is calculated. LV triggers the 6top sublayer to add and release cells to link (i, j) at frame $f + 1$ for $u_{(i,j)}^{f+1} > 0$ and $u_{(i,j)}^{f+1} < 0$, respectively. The value of $u_{(i,j)}^{f+1}$ is calculated as:

$$u_{(i,j)}^{f+1} = \left[\frac{(q_{(i,j)}^f + z_{(i,j)}^{f+1}) \times S}{q_{(i,j)}^f + z_{(i,j)}^{f+1} + \sum_{(l,k) \in N_{i,j}} w_{(i,j,l,k)} (q_{(l,k)}^f + z_{(l,k)}^{f+1})} \right] - p_{(i,j)}^f, \quad (7)$$

where

$$w_{(i,j,l,k)} = \begin{cases} 1, & \text{if } \{i, j\} \cap \{k, l\} \neq \emptyset, \\ 1/M, & \text{otherwise.} \end{cases} \quad (8)$$

The value in the round function in Eq. (7) is the number of cells allocated to link (i, j) at frame f taking into account the new packets from upper layers or neighboring nodes. As we can see from the term $q_{(i,j)}^f$, the number of allocated cells is proportional to the queue length within the neighborhood of link (i, j) , so it leads to semi-equal load between the neighboring links. Also, we scale to the total number of time slots that are needed to transmit all queued packets in the neighborhood of link (i, j) , so that the total number of time slots in the neighborhood is equal to the number of time slots in the frame. The weight $w_{(i,j,l,k)}$ is used to capture the difference between a primary and a secondary conflict. In the first case, since all channels are unavailable to the link, the value is one, but in the second case, since only one of the available channels is blocked,

the value is $1/M$.

The rationale of Eq. (7) can be also seen if we calculate the load at the end of frame $f + 1$. If $q_{(i,j)}^f > p_{(i,j)}^{f+1}$, then we have $x_{(i,j)}^{f+1} = \frac{q_{(i,j)}^{f+1}}{p_{(i,j)}^{f+1}} = \frac{q_{(i,j)}^f - p_{(i,j)}^{f+1} + z_{(i,j)}^{f+1}}{p_{(i,j)}^{f+1}} = \frac{q_{(i,j)}^f + z_{(i,j)}^{f+1}}{p_{(i,j)}^{f+1}} - 1$. In addition, we have that

$$p_{(i,j)}^{f+1} = p_{(i,j)}^f + u_{(i,j)}^{f+1} = \frac{\left(q_{(i,j)}^f + z_{(i,j)}^{f+1}\right) \times S}{q_{(i,j)}^f + z_{(i,j)}^{f+1} + \sum_{(l,k) \in N_{i,j}} w_{(i,j,l,k)} \left(q_{(l,k)}^f + z_{(l,k)}^{f+1}\right)},$$

which means that

$$x_{(i,j)}^{f+1} = \frac{q_{(i,j)}^f + z_{(i,j)}^{f+1} + \sum_{(l,k) \in N_{i,j}} w_{(i,j,l,k)} \left(q_{(l,k)}^f + z_{(l,k)}^{f+1}\right)}{S} - 1.$$

We will show that this quantity is invariant for the links (i, j) and (j, k) that share the same neighborhood. For $\{i, j\} \cap \{k, l\} = \emptyset$, we have

$$x_{(i,j)}^{f+1} = \frac{q_{(i,j)}^f + z_{(i,j)}^{f+1} + \sum_{(l,k) \in N_{i,j}} w_{(i,j,l,k)} \left(q_{(l,k)}^f + z_{(l,k)}^{f+1}\right)}{S} - 1.$$

By substituting (5) into (7), we get

$$u_{(i,j)}^{f+1} = \left[\frac{\left(\max\{0, q_{(i,j)}^f - p_{(i,j)}^{f+1}\} + z_{(i,j)}^f\right) \times S}{\left(\max\{0, q_{(i,j)}^f - p_{(i,j)}^{f+1}\} + z_{(i,j)}^f\right) + \sum_{(l,k) \in N_{i,j}} w_{(i,j,l,k)} \times \left(\max\{0, q_{(l,k)}^f - p_{(l,k)}^{f+1}\} + z_{(l,k)}^f\right)} \right] - p_{(i,j)}^f. \quad (9)$$

4.1. The Local Voting Algorithm

Alg. 1 presents Local Voting algorithm. All links (edges) are examined sequentially at the beginning of each frame. The source node requests for cells, not the receiver. Since we consider a link scheduling scenario, the destination of each transmission is known during the scheduling phase. Every link in the network that has a positive queue length calculates a value u^{f+1} (given in Eq. (7)).

If node n_i has packets to send to node n_j , the value of $u_{(i,j)}^{f+1}$ determines the number of cells that the link (i,j) should ideally gain or release at slot frame $f+1$. If $u_{(i,j)}^{f+1}$ is a positive value, then LV asks from the 6top sublayer to add cells to link (i,j) . Otherwise, if $u_{(i,j)}^{f+1}$ is a negative value, then LV requests from the 6top sublayer to release $u_{(i,j)}^{f+1}$ cells that have been allocated to (i,j) . The cell reallocation should not cause collisions with respect to Eq. (3) and Eq. (4). The collision-free constraint is implemented in 6top sublayer which is responsible for collision-free communication. On the other hand, if node n_i does not have packets to send to destination n_j and cells have been already allocated to link (i,j) in the previous frame, then all allocated cells $p_{(i,j)}^f$ are released. In general, cells are removed from links with a lower load and are offered to links with a higher load.

Algorithm 1 Local Voting

for $(i,j) \in E$ **do** \triangleright Check for all outgoing links (i,j) that originate at node n_i

$qsum_{(i,j)}^{f+1} = (q_{(i,j)}^f + z_{(i,j)}^{f+1}) + \sum_{(l,k) \in N_{i,j}} w_{(i,j,l,k)} \times (q_{(l,k)}^f + z_{(l,k)}^{f+1})$

if $qsum_{(i,j)}^{f+1} \neq 0$ **then** \triangleright Are there packets in the neighborhood of link (i,j) to be sent?

Calculate $u_{(i,j)}^{f+1} = \left\lceil \frac{(q_{(i,j)}^f + z_{(i,j)}^{f+1}) \times S}{qsum_{(i,j)}^{f+1}} \right\rceil - p_{(i,j)}^f$

if $u_{(i,j)}^{f+1} > 0$ **then** \triangleright The link requests cells

Request from 6top to add $u_{(i,j)}^{f+1}$ cells to link (i,j)

else if $u_{(i,j)}^{f+1} < 0$ **then** \triangleright The link releases cells

Request from 6top to delete $u_{(i,j)}^{f+1}$ cells from link (i,j)

end if

else if $p_{(i,j)}^f \neq 0$ **then** \triangleright Are there cells allocated to a link with an empty queue?

Request from 6top to delete $p_{(i,j)}^f$ cells from link (i,j) \triangleright Release the allocated cells

end if

end for

To summarize, LV requests from the 6top sublayer to add cells to link (i, j) at slot frame $f + 1$ when:

- node n_i has packets to send to node n_j and the value of $u_{(i,j)}^{f+1}$ for link (i, j) is positive which means that the link (i, j) has a higher load than its neighbors.

LV requests from the 6top sublayer to release cells from link (i, j) at slot frame $f + 1$ when:

- node n_i has packets to send to node n_j and the value of $u_{(i,j)}^{f+1}$ is negative which means that the link (i, j) has a lower load than its neighbors; or
- node n_i does not have packets to send to node n_j and cells have been already allocated to link (i, j) .

5. Performance Evaluation

The 6TiSCH simulator is an open-source, event-driven Python simulator developed by the members of the 6TiSCH WG [34]. Reference [35] discusses the overall architecture of the 6TiSCH simulator, its use for simulating realistic scenarios, and published results that use the 6TiSCH simulator for different purposes. By default, the simulator supports IEEE 802.15.4e TSCH mode [36], RPL [30], 6top [6], and OTF [10]. In addition to these protocols, we have added Local Voting and Enhanced OTF (E-OTF) algorithms² as part of the work presented in this article. We have implemented two distinct versions of Local Voting, the original version presented in [37], and the modified version presented in this paper. The new version, which is marked as "local_voting_z" in the figures, differs from the original by considering the new packets that are expected to arrive at each slot frame, and not only the current state of the queues of each link as presented with Eq. (7).

²As an online addition to this article, the source code is available at https://github.com/djvergad/local_voting_tsch

We compare the two versions of LV with OTF [10] and E-OTF [11] for two threshold values, 4 and 10 cells. We work with the same simulation parameters as in [10] which have been set according to RFC5673 [5]. The parameters are set according to a) an industrial environment scenario where traffic can be bursty and b) a scenario where traffic is generated at a steady rate.

For the first case, consider a scenario where a leakage is detected in an oil and gas system, the sensors transmit at a higher sample rate in order to minimize the time for detection of the leakage location, to calculate its magnitude, and to estimate the impact and the evolution of the leakage. The simulation parameters are summarized in Table 2.

The simulation scenario considers a network with a grid topology of $2km \times 2km$ where 50 nodes are placed randomly. Every link is associated with a Packet Delivery Rate (PDR) value between 0.00 and 1.00. The PDR value per link is constant during a simulation run. Each node has at least three neighbors where the PDR of the links is at least 50%. A node is moved until this condition is satisfied. The minimum acceptable RSSI value that allows for a packet reception is $-97dBm$, while the maximum number of MAC retries is set to 5. The TSCH schedule contains 101 cells where each time slot has duration of $10ms$.

In the bursty scenario, nodes start to generate data at $20s$ after the beginning of the simulation. Since data is generated in bursts, then the next data generation is at $60s$. We perform simulations where each node generates 1, 5 or 25 packets per burst.

In the steady state scenario the nodes started transmitting at a random time between 16.9 and 33 seconds, and they send at an interval of 0.1, 0.2, or 0.4 seconds, with a uniform random variance of 0.05 times the interval.

The queue length of all nodes is 100 packets. The presented results are averaged over 500 simulation runs. A new topology is used for each run.

The metrics used for performance comparison between LV, OTF and E-OTF are as follows:

- the timestamp for the last packet to reach the root shows the time needed

Table 2: Simulation Setup

Parameter	Value
Number of Nodes	50
Deployment area	square, $2km \times 2km$
Deployment constraint	3 neighbors with $PDR_i \geq 50\%$
Radio sensitivity	$-97dBm$
Max. MAC retries	5
Length of a slot frame	101 cells
Time slot duration	$10ms$
Number of channels	16
Burst timestamp	$20s$ and $60s$
Number of packets per burst	1, 5, 25, 50, and 80 packets per node per burst
Packet inter-arrival interval	0.1, 0.2, and 0.4 seconds
Queue length	100 packets
Number of runs per sample	500
Number of cycles per run	100
6top housekeeping period	$1s$
OTF threshold	4, 10 cells
OTF housekeeping period	$1s$
RPL parents	3

for the two bursts to be completely received by the root;

- the end-to-end latency, defined as the time from a packet generation until

its reception at the sink;

- the energy consumption, calculated by adding the energy of each transmission/reception/idle listen; and
- end-to-end reliability, defined as the ratio between the number of packets received by the sink and the total number of packets sent by all nodes;

Additionally, in order to better explain the evolution of the simulation and to give insights on the reasons for the different performance between the algorithms, we also depict the following values:

- the evolution of the queue fill, defined as the total number of packets in all buffers in the system; and
- the distribution of load in the system, measured using Jain's fairness index and the G-fairness index [38].

5.1. Bursty traffic experiments

In Fig. 3 we can see the timestamp of the last packet that was received for each algorithm and each scenario. In all cases Local Voting and Local Voting z deliver the packets for a shorter time than the other algorithms, with E-OTF achieving the next best performance, and OTF having the worst delay.

Similar results are presented in Fig. 4, where the maximum end-to-end latency is depicted for each algorithm and each scenario. Here we can see that Local Voting and E-OTF have similar performance for scenarios where the load is low, but as the load increases, the advantage of the Local Voting algorithm becomes more apparent.

Regarding the average end-to-end delay (Fig. 5), again Local Voting has the best performance, though the difference is not as prominent as in the previous graphs.

In Figs. 6–9 we can see the evolution over time of the number of packets that have reached the root. In all cases the black and red lines are above the other ones, that indicates that with Local Voting a larger number of packets have

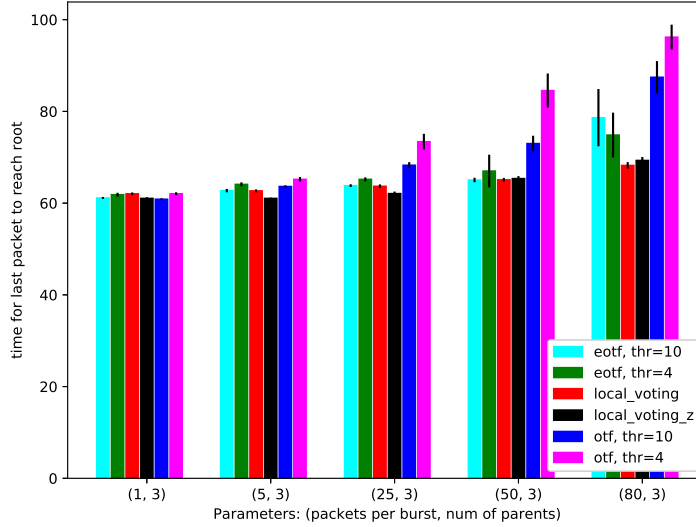


Figure 3: Time for last packet to reach root.

been received at each timestamp. The largest difference appears in Fig. 6, due to the higher traffic load, while the smallest difference is in Fig. 9.

Another important aspect of the performance of the algorithms is the energy that is consumed for the delivering the data to the root. Fig. 10 depicts the energy that is used per received packet, i.e., the fraction of the consumed energy over the number of packets that were successfully delivered to the root. As expected, as the number of packets per burst increases, the energy per packet reduces. We can also see that for small burst sizes OTF has the highest energy consumption per packet, whereas for large burst sizes, E-OTF consumes the most energy per packet. Similar results are depicted in Fig. 11, where the total energy consumption per simulation is depicted. Here the energy consumed increases as the number of packets per burst increase, which is expected, since there are more data transmissions. We show again that for larger numbers of packets per burst, the E-OTF algorithm consumes significantly more energy than the Local Voting and the OTF algorithms. The evolution of the energy

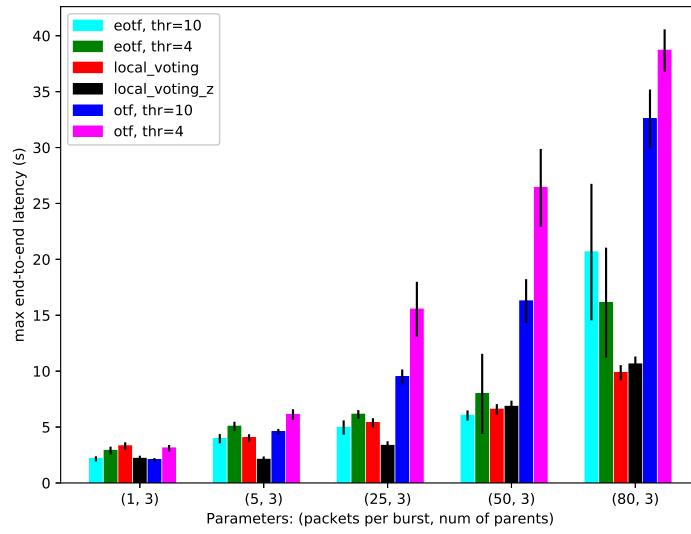


Figure 4: Maximum end-to-end latency.

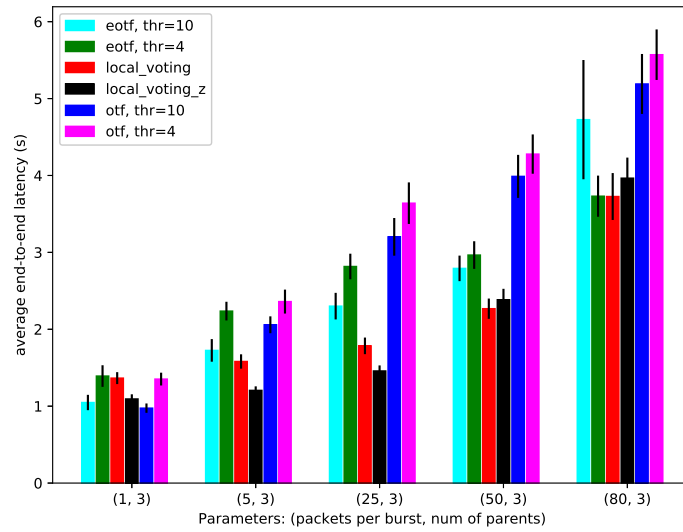


Figure 5: Average end-to-end latency.

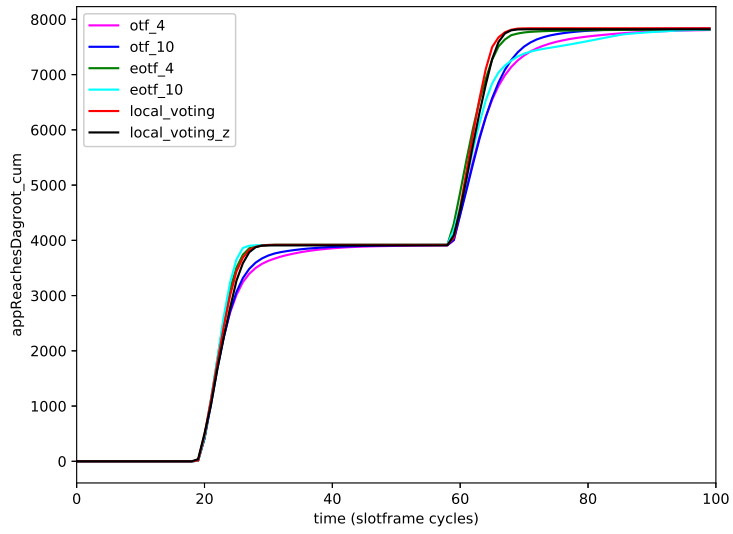


Figure 6: Number of packets that reach the root as a function of time, 80 packets per burst.

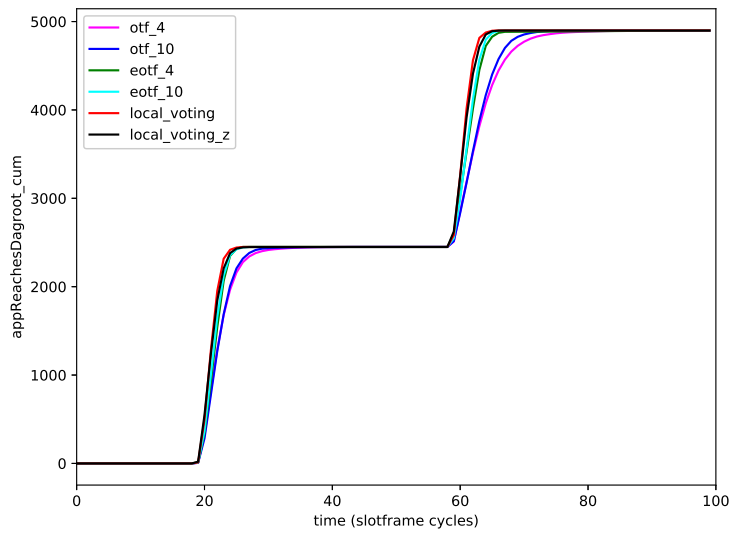


Figure 7: Number of packets that reach the root as a function of time, 50 packets per burst.

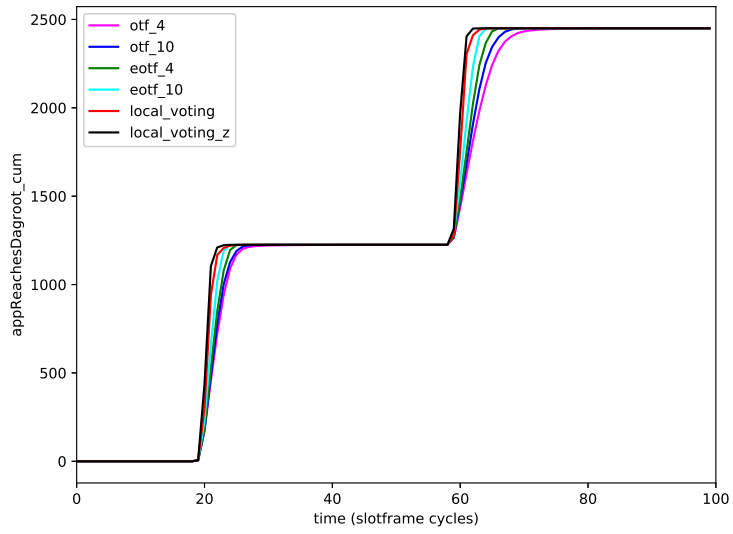


Figure 8: Number of packets that reach the root as a function of time, 25 packets per burst.

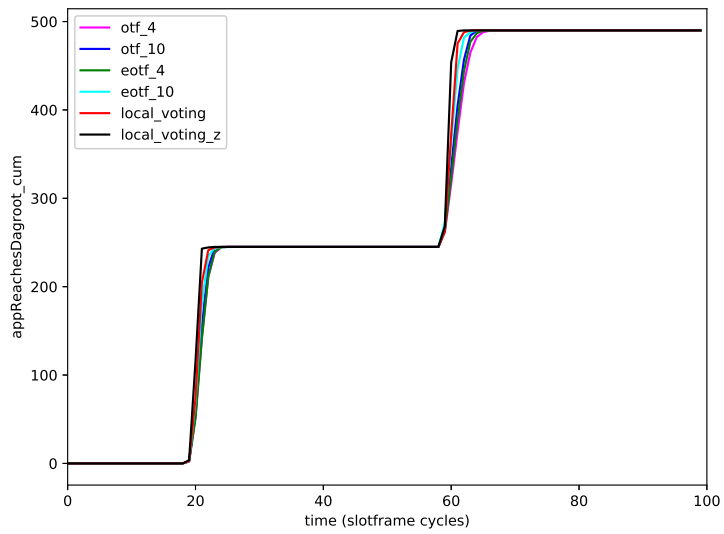


Figure 9: Number of packets that reach the root as a function of time, 5 packets per burst.

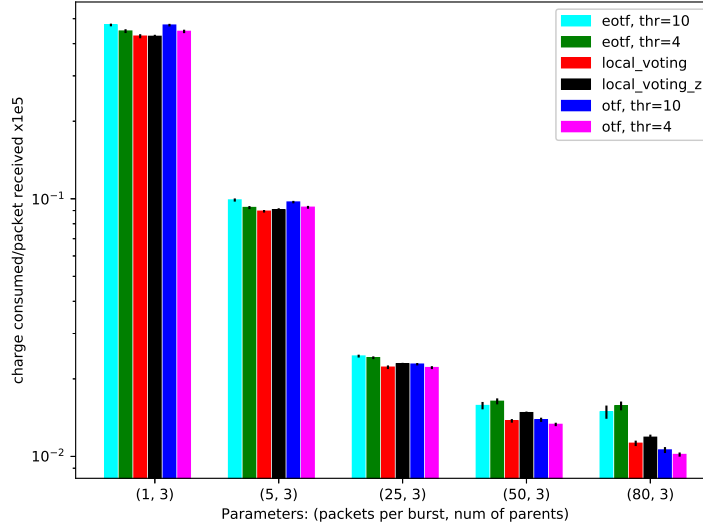


Figure 10: Energy consumption per received packet.

consumption over time is given in Figs. 12–15. This confirms that E-OTF uses more energy than the other algorithms, whereas Local Voting and OTF have similar consumption. The conclusion is that Local Voting has performance in terms of delay similar to E-OTF, but with an energy consumption similar to OTF, so it combines both good delay performance and energy efficiency.

Fig. 16 shows the average queue sizes among all nodes in the network during the entire simulation, for each algorithm and for each scenario. A more detailed view is available in Figs. 17–19, where it is evident that the increased efficiency of Local Voting makes the queue sizes to be reduced more rapidly and all of the packets to reach their destinations faster. In all cases the Local Voting algorithm achieves the smallest queue sizes, which is the reason that it exhibits lower delay than the other algorithms. This smaller queue size is also the reason behind the increased reliability of the Local Voting algorithm compared to OTF and E-OTF.

In Fig. 20–23, we can see the average fairness between the nodes in the

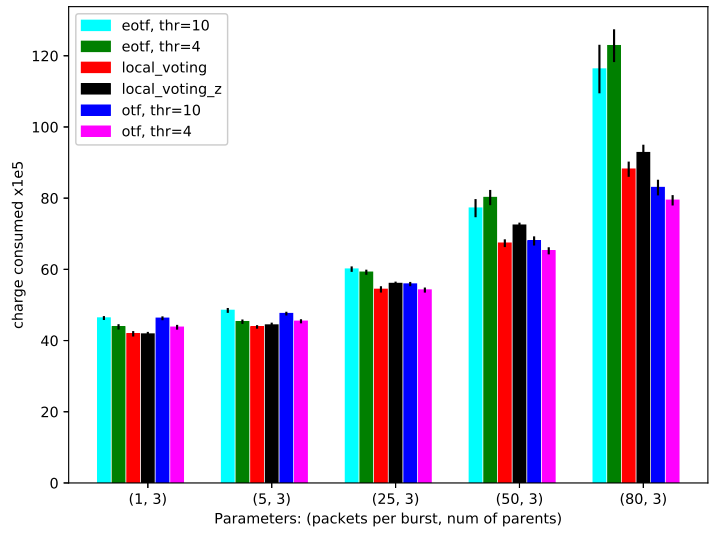


Figure 11: Energy consumption

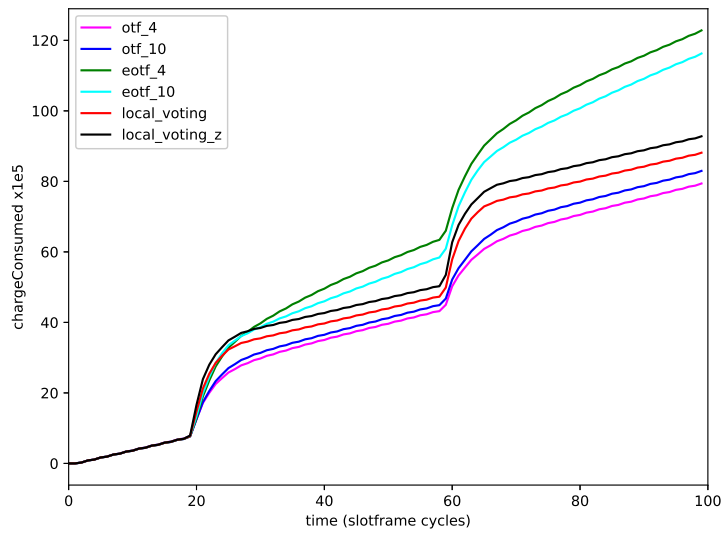


Figure 12: Evolution of the energy consumption over time, 80 packets per burst

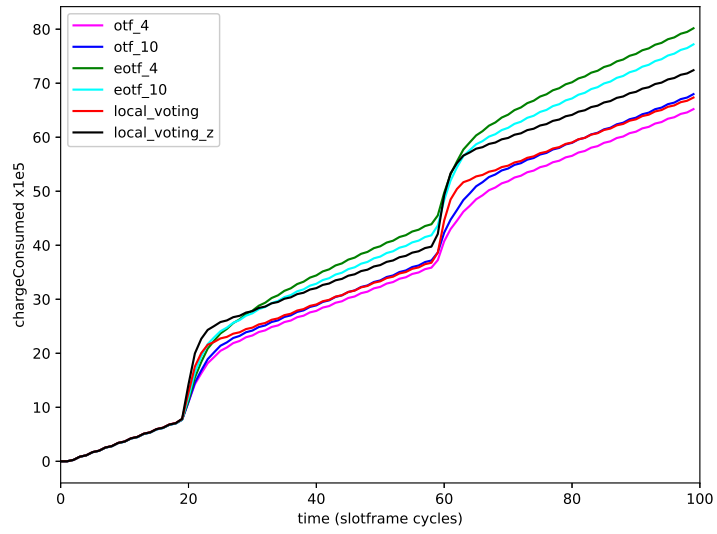


Figure 13: Evolution of the energy consumption over time, 50 packets per burst

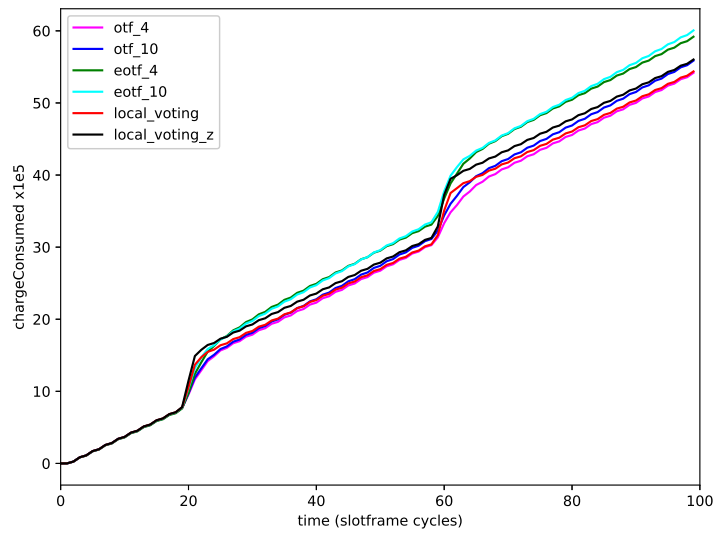


Figure 14: Evolution of the energy consumption over time, 25 packets per burst

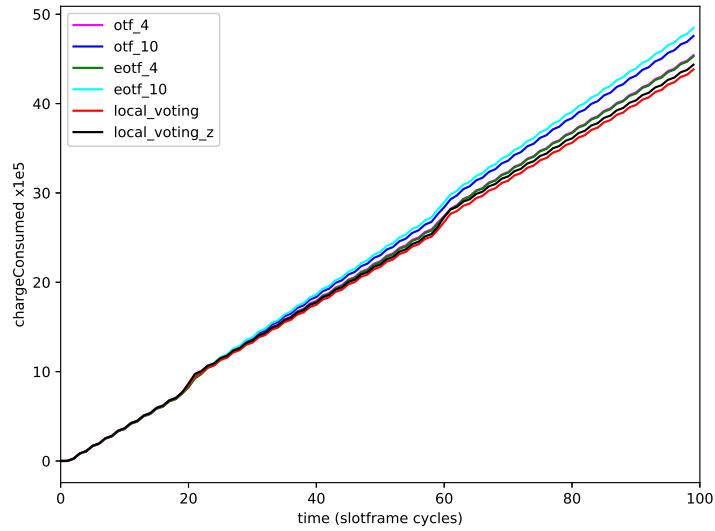


Figure 15: Evolution of the energy consumption over time, 5 packets per burst

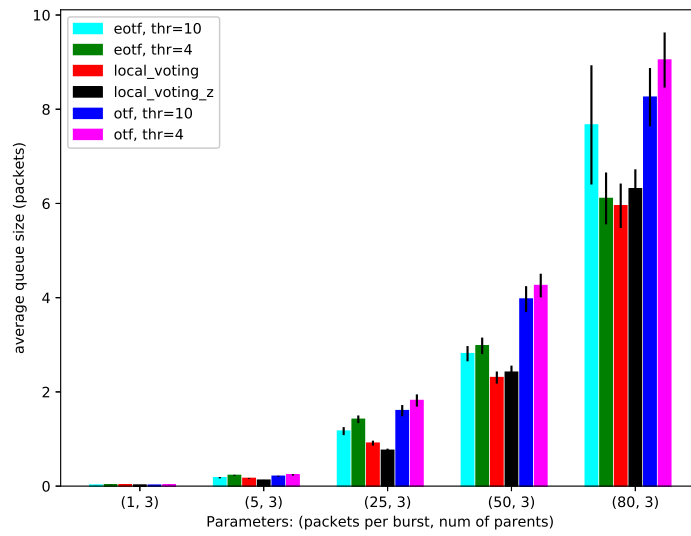


Figure 16: Average queue size (packets) for the entire simulation.

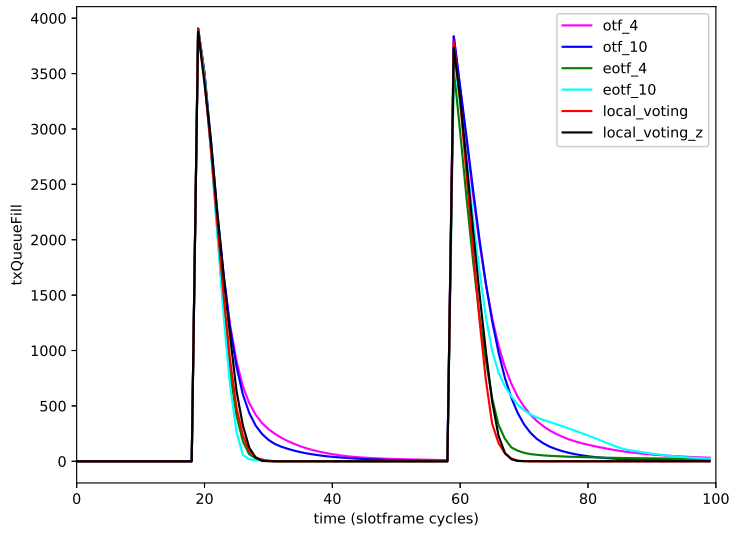


Figure 17: Evolution over time, 80 packets per burst.

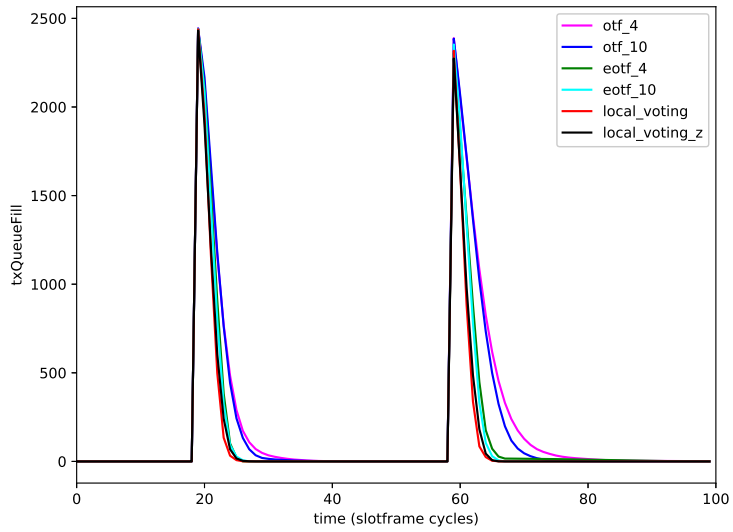


Figure 18: Evolution over time, 50 packets per burst.

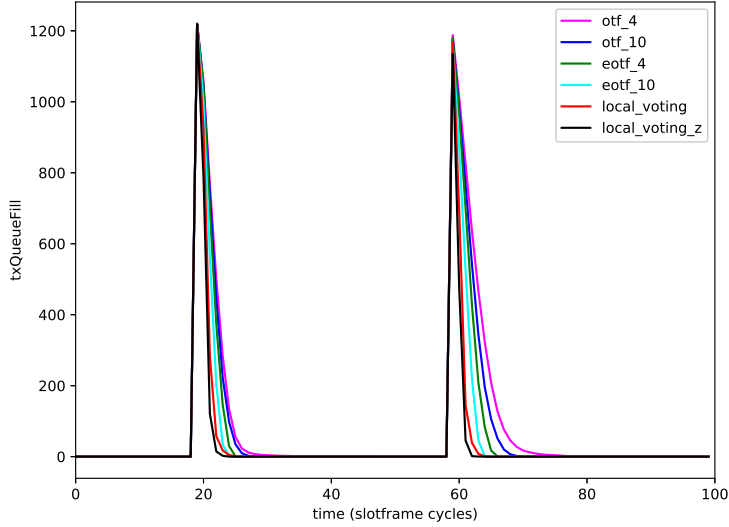


Figure 19: Evolution over time, 25 packets per burst.

network, calculated on the load of each node (i.e. the ratio of queue length over slot allocation), using two fairness metrics, namely Jain’s fairness index and the G fairness index. The local voting algorithm has the best fairness in terms of load, which is expected, since by design it tries to equalize the load throughout the congested areas of the network.

5.2. Uniform traffic experiments

This subsection contains the results of the uniform traffic experiment, where the nodes transmit at a constant rate, with some variability in the traffic generation time to avoid synchronization issues.

In Fig. 24 we can see the maximum latency for each scenario. We can see that in this scenario the advantage of local voting z over the previous version of local voting in terms of maximal delay. Specifically, local voting z has the smallest maximum delay compared to all the other algorithms. This can be explained, since for local voting a large queue is necessary for increasing the

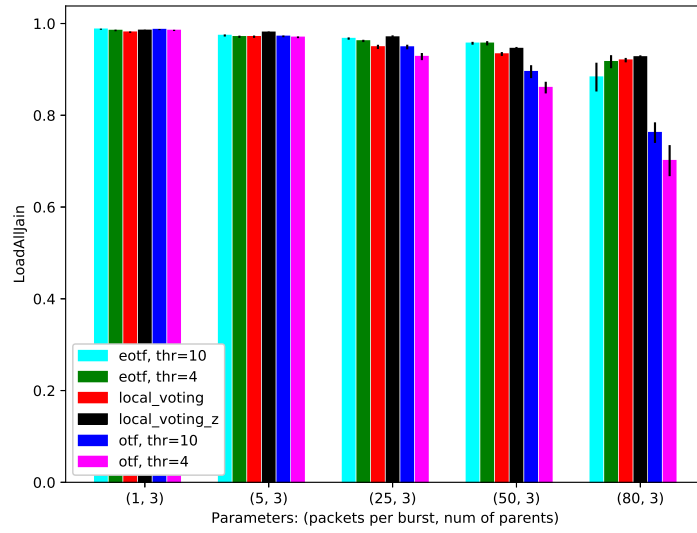


Figure 20: Fairness in load distribution, with Jain's fairness index, average.

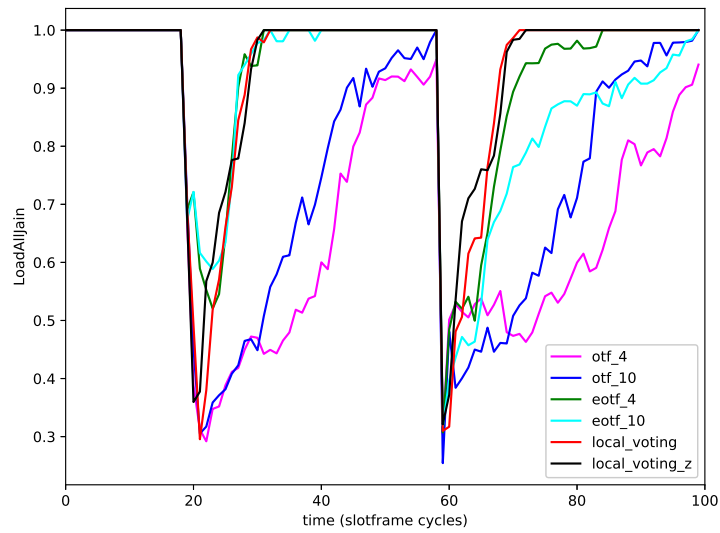


Figure 21: Fairness in load distribution, with Jain's fairness index, over time, 80 packets per burst.

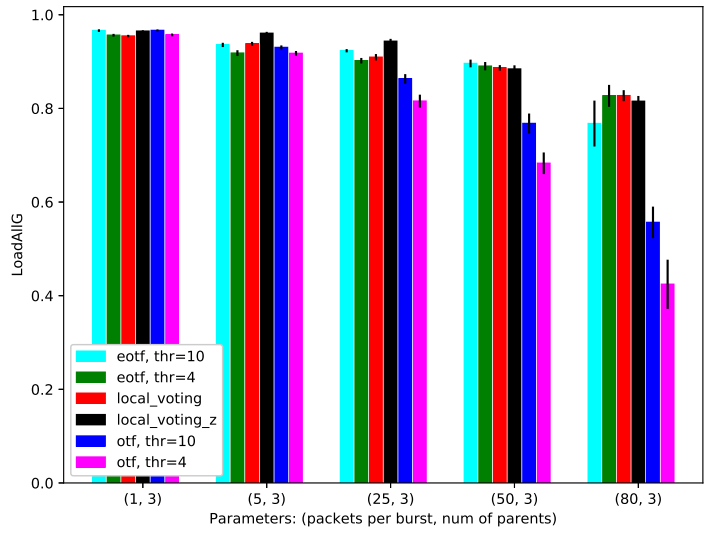


Figure 22: Fairness in load distribution, with G fairness index, average.

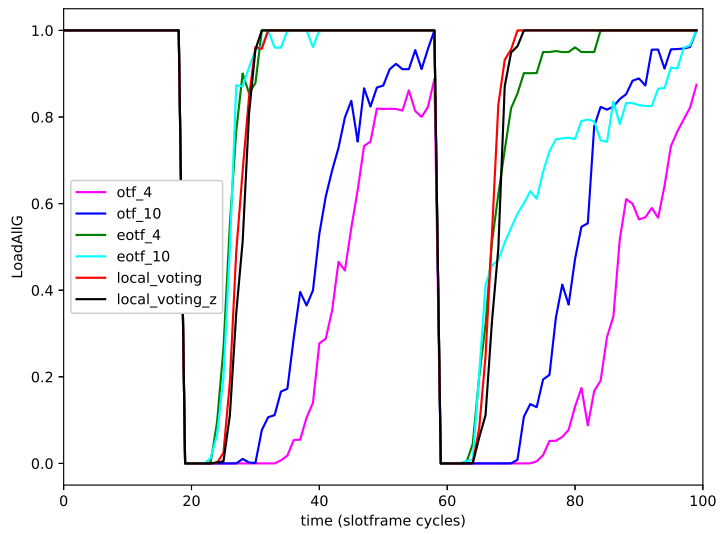


Figure 23: Fairness in load distribution, with G fairness index, over time, 80 packets per burst.

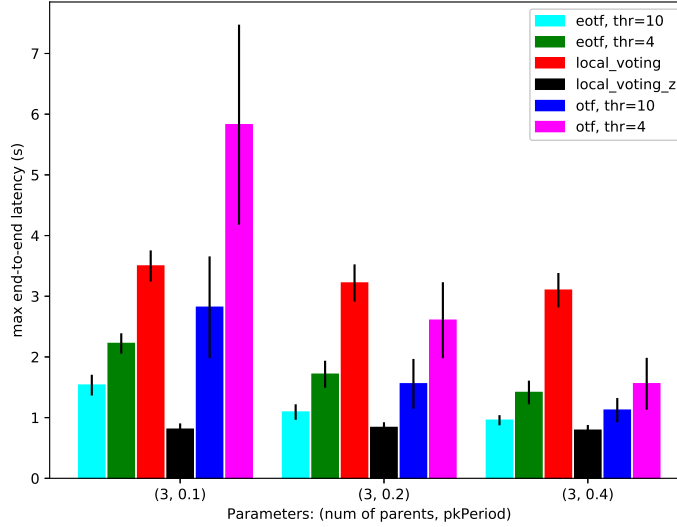


Figure 24: The maximum average latency for the different scenarios.

slot allocation, whereas in the case of local voting z , the slot allocation also tracks the new packets that are generated at each round, so that the buffer-bloat problem can be avoided. In a sense local voting z considers the ongoing rate of traffic that must be delivered, in addition to the current buffer size, whereas local voting (without z) only considers the buffer. The difference is even more apparent in Fig. 25, where the average latency is depicted.

The evolution over the latency over time may be seen in Fig.26. Similar results are available for the other scenarios as well.

However, the improved performance in terms of latency comes at a cost of larger energy consumption (Fig. 27, 28).

The reliability of all algorithms except OTF was perfect in all cases (Fig. 29).

The lower delay of the local voting z algorithm can be easily explained by seeing Fig. 30, Fig. 31, and Fig. 32, where it is apparent that the queue sizes are much smaller for local voting z , resulting in the reduction of the latency.

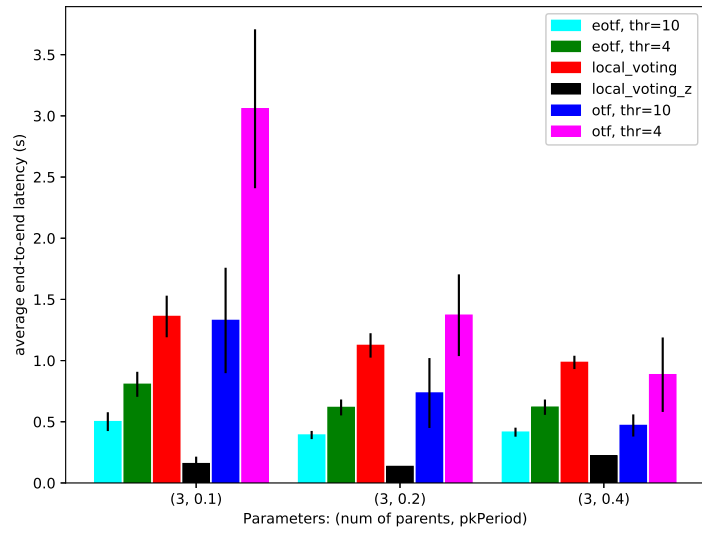


Figure 25: The average latency for the different scenarios.

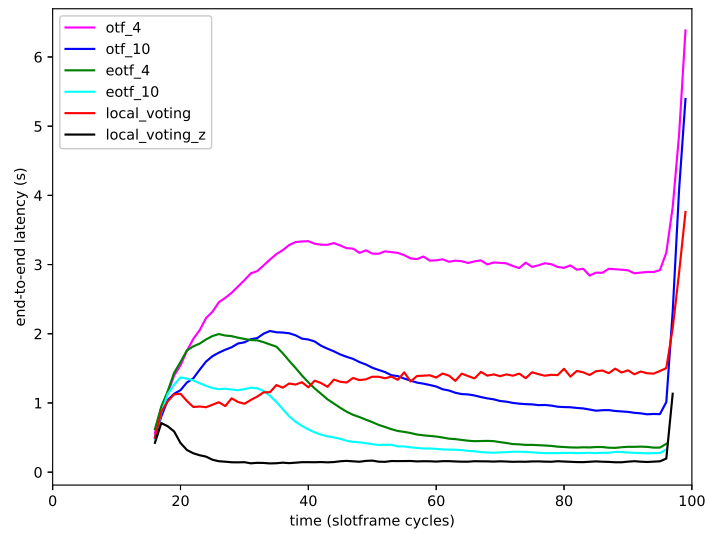


Figure 26: The average latency over time for an packet inter-arrival time of 0.1 seconds.

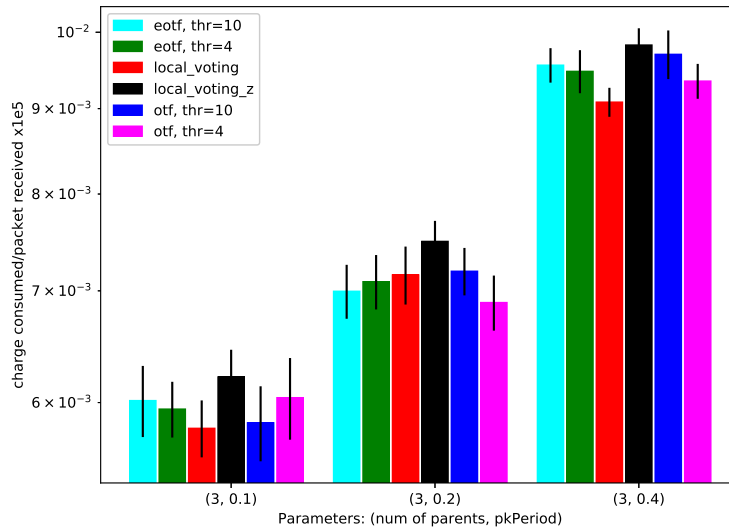


Figure 27: The charge consumed per received packet for the different scenarios.

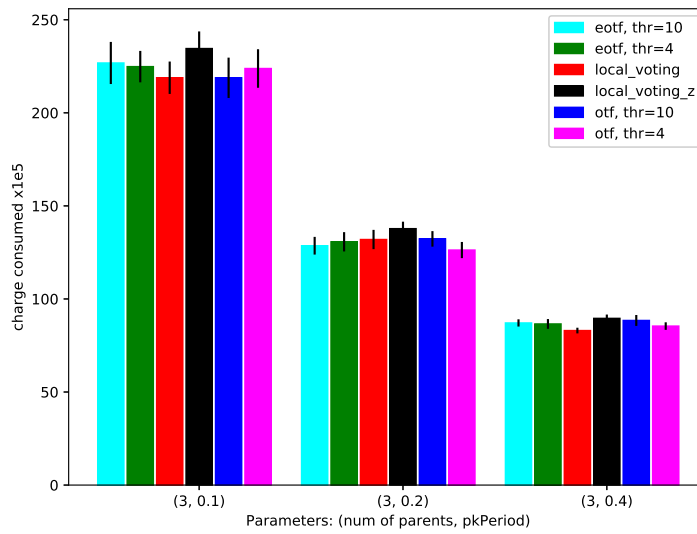


Figure 28: The total charge consumed for the different scenarios.

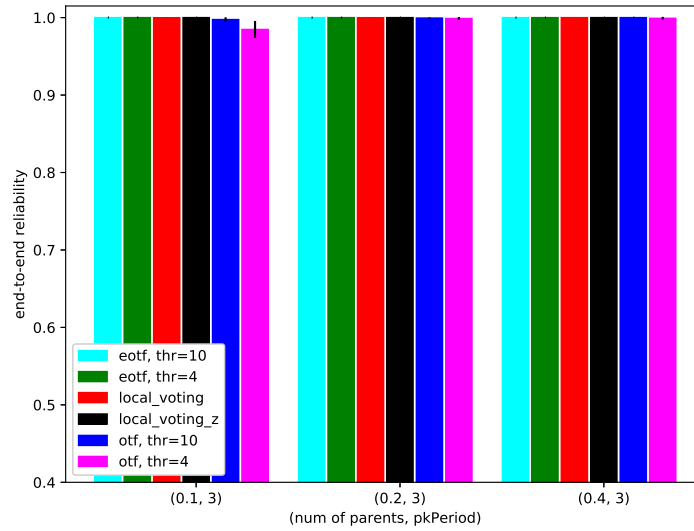


Figure 29: The reliability (ratio of generated packets that reach their destination) for the different scenarios.

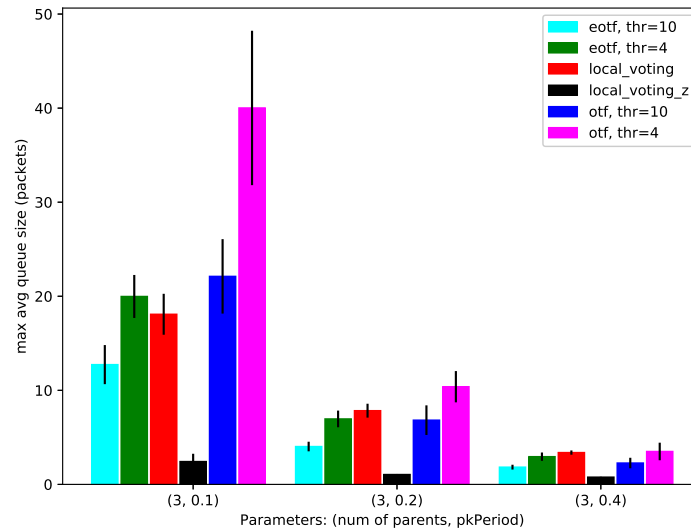


Figure 30: The maximum average queue size for the different scenarios.

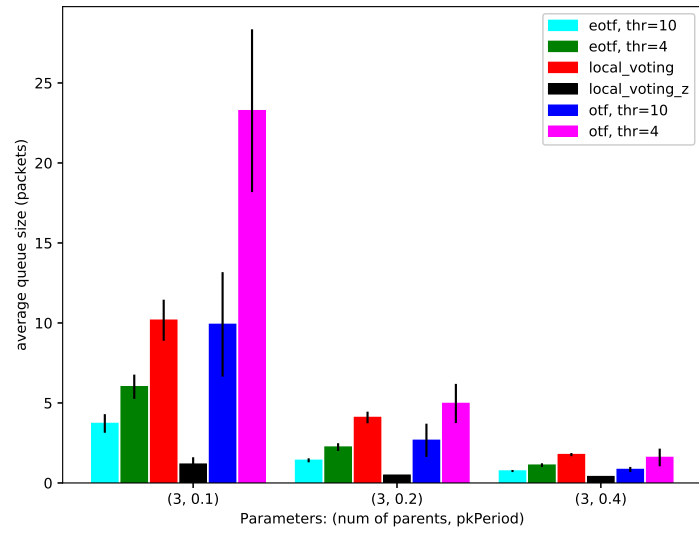


Figure 31: The average queue size for the different scenarios.

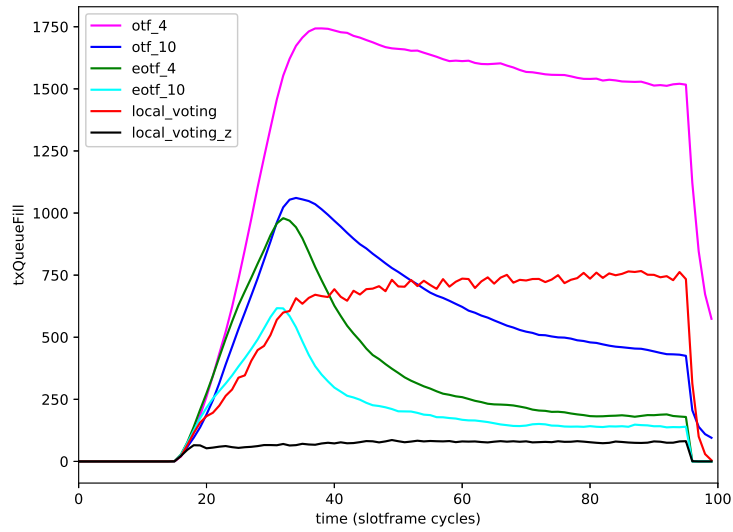


Figure 32: The average queue size over time for an packet inter-arrival time of 0.1 seconds.

Additional results are available at github repository³, that are omitted in this paper due to space limitations.

6. Conclusions

We proposed a new distributed bandwidth reservation algorithm called *Local Voting* which balances the load between links in 6TiSCH networks. The algorithm calculates the number of cells to be added or released by 6top while considering the collision-free constraints. In this way, it adapts the schedule to the network conditions in 6TiSCH networks, equalizes the load in congested areas, that as expected provides efficient resource allocation. We showed that optimal schedules are maximal and balanced, and these are the two design goals of LV. Extensive simulation results show that LV combines the good delay performance of E-OTF and the energy efficiency of OTF, while outperforming them in terms of reliability and fairness. To summarize, we proved the advantage of load balancing when performing link scheduling in 6TiSCH networks, proposed Local Voting for distributed bandwidth reservation in 6TiSCH networks, and we demonstrated by simulations that the Local Voting algorithm shows an overall very good performance in comparison with other state-of-the-art algorithms. In addition, the new variant of the algorithm, named *local voting z*, achieves lower latency than the other algorithms we compared with, even in the steady-state scenario.

References

References

- [1] L. Atzori, A. Iera, G. Morabito, The internet of things: A survey, *Computer Networks* 54 (15) (2010) 2787 – 2805.

³As an online addition to this article, the source code is available at https://github.com/djvergad/local_voting_tsch

doi:<http://dx.doi.org/10.1016/j.comnet.2010.05.010>.

URL <http://www.sciencedirect.com/science/article/pii/S1389128610001568>

- [2] D. Evans, The internet of things how the next evolution of the internet is changing everything, Cisco 1.
- [3] D. Guglielmo, G. Anastasi, A. Seghetti, From ieee 802.15.4 to ieee 802.15.4e: A step towards the internet of things, in: Advances onto the Internet of Things, Vol. 260, Springer, 2014, pp. 135–152.
- [4] T. Watteyne, M. R. Palattella, L. A. Grieco, Using IEEE 802.15.4e Time-Slotted Channel Hopping (TSCH) in the Internet of Things (IoT): Problem RFC 7554 (May 2015). doi:10.17487/rfc7554.
URL <https://rfc-editor.org/rfc/rfc7554.txt>
- [5] K. Pister, P. Thubert, S. Dwars, T. Phinney, Industrial Routing Requirements in Low-Power and Lossy Networks, IETF Standard RFC 5673 (2009). doi:10.17487/rfc7554.
URL <https://rfc-editor.org/rfc/rfc7554.txt>
- [6] Q. Wang, X. Vilajosana, 6TiSCH Operation Sublayer (6top), Internet-draft, Internet Engineering Task Force, work in Progress (Nov. 2015).
- [7] Q. Wang, X. Vilajosana, T. Watteyne, 6TiSCH Operation Sublayer Protocol (6P), Internet-Draft draft-ietf-6tisch-6top-protocol-12, Internet Engineering Task Force, work in Progress (Jun. 2018).
URL <https://datatracker.ietf.org/doc/html/draft-ietf-6tisch-6top-protocol-12>
- [8] D. J. Vergados, N. Amelina, Y. Jiang, K. Krlevska, O. Granichin, Towards optimal distributed node scheduling in a multihop wireless network through local voting, IEEE Transactions on Wireless Communications 17 (1) (2018) 400–414. doi:10.1109/TWC.2017.2767045.
- [9] D. J. Vergados, N. Amelina, Y. Jiang, K. Krlevska, O. Granichin, Local voting: Optimal distributed node scheduling algorithm for mul-

- tihop wireless networks, in: IEEE Conf. on Computer Communications Workshops (INFOCOM WKSHPS), 2017, pp. 1014–1015. doi:10.1109/INFOCOMW.2017.8116537.
- [10] M. R. Palattella, T. Watteyne, Q. Wang, K. Muraoka, N. Accettura, D. Dujovne, L. A. Grieco, T. Engel, On-the-fly bandwidth reservation for 6tisch wireless industrial networks, IEEE Sensors Journal 16 (2) (2016) 550–560. doi:10.1109/JSEN.2015.2480886.
- [11] F. Righetti, C. Vallati, G. Anastasi, S. K. Das, Analysis and improvement of the on-the-fly bandwidth reservation algorithm for 6tisch, in: IEEE 19th International Symposium on "A World of Wireless, Mobile and Multimedia Networks" (WoWMoM), 2018, pp. 1–9. doi:10.1109/WoWMoM.2018.8449793.
- [12] M. R. Palattella, N. Accettura, M. Dohler, L. A. Grieco, G. Boggia, Traffic aware scheduling algorithm for reliable low-power multi-hop iee 802.15.4e networks, in: 2012 IEEE 23rd International Symposium on Personal, Indoor and Mobile Radio Communications - (PIMRC), 2012, pp. 327–332. doi:10.1109/PIMRC.2012.6362805.
- [13] A. Tinka, T. Watteyne, K. Pister, A decentralized scheduling algorithm for time synchronized channel hopping, in: J. Zheng, D. Simplot-Ryl, V. C. M. Leung (Eds.), Ad Hoc Networks, Springer Berlin Heidelberg, Berlin, Heidelberg, 2010, pp. 201–216.
- [14] N. Accettura, E. Vogli, M. R. Palattella, L. A. Grieco, G. Boggia, M. Dohler, Decentralized traffic aware scheduling in 6tisch networks: Design and experimental evaluation, IEEE Internet of Things Journal 2 (6) (2015) 455–470. doi:10.1109/JIOT.2015.2476915.
- [15] S. Duquennoy, B. Al Nahas, O. Landsiedel, T. Watteyne, Orchestra: Robust mesh networks through autonomously scheduled tsch, in: Proceedings of the 13th ACM Conference on Embedded Networked

Sensor Systems, SenSys '15, ACM, New York, NY, USA, 2015, pp. 337–350. doi:10.1145/2809695.2809714.
URL <http://doi.acm.org/10.1145/2809695.2809714>

- [16] E. Municio, S. Latré, Decentralized broadcast-based scheduling for dense multi-hop tsch networks, in: Proc. of the Workshop on Mobility in the Evolving Internet Architecture, 2016, pp. 19–24. doi:10.1145/2980137.2980143.
URL <http://doi.acm.org/10.1145/2980137.2980143>
- [17] R. H. Hwang, C. C. Wang, W. B. Wang, A distributed scheduling algorithm for ieee 802.15.4e wireless sensor networks, Comput. Stand. Interfaces 52 (C) (2017) 63–70. doi:10.1016/j.csi.2017.01.003.
URL <https://doi.org/10.1016/j.csi.2017.01.003>
- [18] M. A. Kafi, J. B. Othman, A. Ouadjaout, M. Baga, N. Badache, Refiacc: Reliable, efficient, fair and interference-aware congestion control protocol for wireless sensor networks, Computer Communications 101 (2017) 1 – 11. doi:<https://doi.org/10.1016/j.comcom.2016.05.018>.
URL <http://www.sciencedirect.com/science/article/pii/S0140366416302353>
- [19] K. Muraoka, T. Watteyne, N. Accettura, X. Vilajosana, K. S. J. Pister, Simple distributed scheduling with collision detection in tsch networks, IEEE Sensors Journal 16 (15) (2016) 5848–5849. doi:10.1109/JSEN.2016.2572961.
- [20] T. P. Duy, T. Dinh, Y. Kim, Distributed cell selection for scheduling function in 6tisch networks, Comput. Stand. Interfaces 53 (C) (2017) 80–88. doi:10.1016/j.csi.2017.03.008.
URL <https://doi.org/10.1016/j.csi.2017.03.008>
- [21] R. Soua, P. Minet, E. Livolant, Wave: A distributed scheduling algorithm for convergecast in ieee 802.15.4, Trans. Emerg. Telecommun. Technol. 27 (4) (2016) 557–575. doi:10.1002/ett.2991.
URL <https://doi.org/10.1002/ett.2991>

- [22] R. Soua, P. Minet, E. Livolant, DiSCA: A distributed scheduling for convergecast in multichannel wireless networks, in: IFIP/IEEE International Symposium on Integrated Network Management, IM 2015, Ottawa, ON, Canada, 11-15 May, 2015, 2015, pp. 156–164.
URL <http://ieeexplore.ieee.org/xpl/mostRecentIssue.jsp?punumber=7121095>
- [23] A. Aijaz, U. Raza, Deamon: A decentralized adaptive multi-hop scheduling protocol for 6tisch wireless networks, *IEEE Sensors Journal* 17 (20) (2017) 6825–6836. doi:10.1109/JSEN.2017.2746183.
- [24] G. Daneels, B. Spinnewyn, S. Latre, J. Famaey, Resf: Recurrent low-latency scheduling in IEEE 802.15.4e TSCH networks, *Ad Hoc Networks* 69 (2018) 100 – 114.
doi:<https://doi.org/10.1016/j.adhoc.2017.11.002>.
URL <http://www.sciencedirect.com/science/article/pii/S1570870517302019>
- [25] D. Dujovne, L. A. Grieco, M. R. Palattella, N. Accettura, 6TiSCH 6top Scheduling Function Zero (SF0), Internet-draft, Internet Engineering Task Force, work in Progress (Mar. 2016).
URL <https://datatracker.ietf.org/doc/html/draft-dujovne-6tisch-6top-sf0-01>
- [26] T. Chang, T. Watteyne, X. Vilajosana, Q. Wang, Ccr: Cost-aware cell relocation in 6tisch networks, *Transactions on Emerging Telecommunications Technologies* 29 (1) (2018) e3211.
arXiv:<https://onlinelibrary.wiley.com/doi/pdf/10.1002/ett.3211>,
doi:10.1002/ett.3211.
URL <https://onlinelibrary.wiley.com/doi/abs/10.1002/ett.3211>
- [27] D. Guglielmo, S. Brienza, G. Anastasi, *Ieee 802.15.4e: A survey*, *Computer Communications* 88 (2016) 1 – 24.
doi:<http://dx.doi.org/10.1016/j.comcom.2016.05.004>.
URL <http://www.sciencedirect.com/science/article/pii/S0140366416301980>
- [28] R. Hermeto, A. Gallais, F. Theoleyre, Scheduling for IEEE802.15.4-TSCH and slow channel hopping MAC in low power industrial wireless networks

Computer Communications 114 (2017) 84 – 105.

doi:<https://doi.org/10.1016/j.comcom.2017.10.004>.

URL <http://www.sciencedirect.com/science/article/pii/S0140366417301147>

- [29] S. Kharb, A. Singhrova, A survey on network formation and scheduling algorithms for time slotted channels, *Journal of Network and Computer Applications* 126 (2019) 59 – 87.
doi:<https://doi.org/10.1016/j.jnca.2018.11.004>.
URL <http://www.sciencedirect.com/science/article/pii/S1084804518303631>
- [30] T. W. et al., RPL: IPv6 Routing Protocol for Low-Power and Lossy Networks, RFC 6550 (Mar. 2012). doi:[10.17487/rfc6550](https://doi.org/10.17487/rfc6550).
URL <https://rfc-editor.org/rfc/rfc6550.txt>
- [31] T. Watteyne, M. R. Palattella, L. A. Grieco, Using IEEE 802.15.4e Time-Slotted Channel Hopping (TSCH) in the Internet of Things (IoT): Problem Statement and Internet Engineering Task Force.
URL <https://hal.inria.fr/hal-01208395>
- [32] A. Morell, X. Vilajosana, J. L. Vicario, T. Watteyne, Label switching over IEEE802.15.4e networks, *Trans. Emerging Telecommunications Technologies* 24 (5) (2013) 458–475.
URL <http://dx.doi.org/10.1002/ett.2650>
- [33] N. Amelina, A. Fradkov, Y. Jiang, D. J. Vergados, Approximate consensus in stochastic networks with application to load balancing, *IEEE Trans. on Information Theory* 61 (4) (2015) 1739–1752.
doi:[10.1109/TIT.2015.2406323](https://doi.org/10.1109/TIT.2015.2406323).
- [34] T. Watteyne, K. Muraoka, N. Accettura, X. Vilajosana, The 6tisch simulator, <https://bitbucket.org/6tisch/simulator/src>.
- [35] E. Municio, G. Daneels, M. Vučinić, S. Latré, J. Famaey, Y. Tanaka, K. Brun, K. Muraoka, X. Vilajosana, T. Watteyne, Simulating 6tisch networks, *Transactions on Emerging Telecommunications Technologies* (2018) e3494.

- [36] IEEE, IEEE Standard for Local and Metropolitan Area Networks-Part 15.4: Low-Rate Wireless Personal Area Networks (LR-WPANs) Amendment 1: MAC Sublayer, IEEE Std 802.15.4e-2012 (Apr. 2012).
- [37] K. Krlevska, D. J. Vergados, Y. Jiang, A. Michalas, A load balancing algorithm for resource allocation in iee 802.15.4e networks, in: IEEE International Conference on Pervasive Computing and Communications Workshops (PerCom Workshops), 2018, pp. 675–680. doi:10.1109/PERCOMW.2018.8480306.
- [38] Wikipedia, Fairness measure — Wikipedia, the free encyclopedia, <http://en.wikipedia.org/w/index.php?title=Fairness%20measure&oldid=847782798>, [Online; accessed 16-December-2018] (2018).